BNL-NUREG-32124
Conf-821037--62

BNL-NUREG--32124

DE83 003962

BNL PROGRAM IN SUPPORT OF LWR DEGRADED-CORE ACCIDENT ANALYSIS

by

T. Ginsberg and G. A. Greene

Program Contributors: J. Klages, J. Klein, C. E. Schwarz, Y. Sanborn, N. Tutu

Consultants: J. C. Chen, T. F. Irvine

Brookhaven National Laboratory
Department of Nuclear Energy
Experimental Modeling Group
Upton, NY 11973

Presented at the

Tenth Water Reactor Safety Research Information Meeting
October 12-15, 1982
Gaithersburg, Maryland

BNL PROGRAM IN SUPPORT OF LWR DEGRADED CORE ACCIDENT ANALYSIS

T. Ginsberg and G. A. Greene

1. INTRODUCTION

The U.S. Nuclear Regulatory Commission currently sponsors analyses of the response of light water reactor containment buildings to degraded core accidents (Murfur, 1980; Meyer, 1981; Pratt, 1981). Two major sources of loading on dry pressurized water reactor containments are:

(i) Steam generation from core debris water thermal interactions.

Quenching of hot debris by cooling water leads to steam generation and containment pressurization. Interaction of hot, unquenched debris with concrete can lead to simultaneous gas release. Hydrogen continues to be generated until debris is finally quenched.

(ii) Molten core-concrete interactions.

The interactions lead to pressurization of the containment as a result of generation of concrete decomposition products and potential combustion of flammable gaseous products. In addition these interactions lead to penetration of the core melt into the containment basemat.

Experiments are in progress at BNL in support of analytical model development related to aspects of the above containment loading mechanisms. The work supports development and evaluation of the CORCON (Muir, 1981) and MARCH (Wooton, 1980) computer codes. Progress in the two programs is described below.

2. CORE DEBRIS THERMAL-HYDRAULIC PHENOMENOLOGY

Light water reactor degraded core accident sequence studies have been performed which postulate the existence of a high temperature core debris bed within the reactor cavity (Meyer, 1981). The debris bed would be cooled by an overlying pool of water. Two models have been used to characterize the interaction between hot core debris and water. The MARCH code's "HOTDROP" model (Wooton, 1980) assumes that the core debris is suspended in an infinite sea of water and that heat transfer is limited by the particle debris internal and external thermal resistances. Steam production is governed by the total surface area of the fragments. On the other hand, steady state debris bed cooling models have been used to predict the steam production rate resulting from quenching of packed beds of solid core debris (Yang, 1981). The containment pressurization rates based upon the two models are significantly different (Yang, 1981). The validity of these models when applied to the transient cooling of debris beds has not been established by comparison with suitable

transient quench experiments.

Presented below are recent results of an experimental investigation whose objective is to provide an understanding of the thermal interaction between superheated core debris and water during postulated light water reactor degraded core accidents. The experiment was designed to study the heat transfer characteristics of superheated spheres as they are quenched in a packed bed configuration by an overlying pool of water. A model based upon the experimental results is presented and implications with respect to reactor safety are discussed.

The test apparatus is shown in Figure 1. Stainless steel spheres, 3 mm in diameter, were heated in the oven shown at the top of Figure 1 to temperatures between 533 K and 977 K. They were subsequently transferred to a vertical 108.2 mm i.d. stainless steel pipe, flanged at the lower end. Water at temperatures between 274 K and 360 K was released on to the spheres and the resulting thermal interaction was observed. Packed beds of 40% porosity were studied, whose nominal heights were in the range 200 mm to 400 mm. The experiments were carried out at constant pressure, with the steam vented to the atmosphere. The wall of the test vessel could be preheated, if desired, to match the initial sphere temperature. The test section was instrumented with an array of thermocouples, both within the pipe and on its outside wall. A pressure transducer was mounted on the test vessel wall to monitor pressure fluctuations indicative of continued boiling within the vessel. In the early stages of the work the steam was vented to the atmosphere via the steam vent shown in Figure 1. The apparatus was subsequently modified to incorporate the turbine flowmeter shown in Figure 1(b). This flowmeter was used to monitor the flow of steam during the particle quench process. In these latter experiments all of the piping which led to the flowmeter was preheated to the water saturation temperature prior to a run.

A typical set of bed temperature traces is shown for Run. No. 116 in Figure 2. The temperature traces are labeled by the thermocouple (TC) identification number. TC2 was located at the base of the bed. The remaining thermocouples were spaced in ascending order every 50 mm. TC8 was the uppermost thermocouple located 300 mm from the base of the bed. The key feature of Figure 2 is the sequence of step changes in temperature, beginning with TC8 located near the top of the bed. This sequence proceeded in the downward direction to each thermocouple in the bed. The temperature at each position suddenly fell from the initial sphere temperature to the liquid saturation temperature. Figure 2 also indicates that several of the thermocouples partially recovered their superheated temperatures subsequent to the first arrival of liquid. In this case four channels (TC Nos. 4, 6, 7, 8) exhibit this behavior. The temperature recovery characteristic of Run No. 116 occurred in many, though not all, of the experiments. These four thermocouples were finally quenched in a sequential pattern from the bottom upwards. A sequential pattern of wall quenching was also observed to proceed from the bottom upwards (not shown).

Three "frontal" particle bed cooling patterns are suggested by the bed and wall temperature traces. The times of arrival of each of the three cooling fronts are presented in Figure 3 as a function of axial position in the test column. Figure 3 shows the advance of a downward-propagating front which

reaches the bottom of the bed at 165 seconds after initial water/bed contact. At this point an upward-propagating front is observed which is responsible for "final" cooling of the particle bed as well as the test wall (third front was wall quench).

Prior to installation of the turbine flowmeter system for the steam flowrate measurement, an estimate of the time-average bed heat transfer rate was made. The time period during which boiling was observed in the test vessel was determined from the piezoelectric transducer traces.

The average bed heat flux was computed from the known initial bed stored energy (temperature), the boiling time and the bed cross-sectional area. The results of these calculations are shown in Figure 4. They indicate that the time-average rate of heat transfer from the particles to the water was approximately 10^6 W/m^2. The heat transfer rate was independent of bed temperature for initial bed temperatures in the range 530 K to 970 K.

The turbine flowmeter data substantiate the magnitude of the heat flux determined as described above. In addition the flowmeter data indicate that the bed cooling rate is identical during the downward and upward frontal time periods.

The frontal progression speeds were obtained from the frontal propagation data (such as Figure 3) for each set of experimental conditions. These data, calculated using a linear least squares analysis, are shown in Figure 5. Data from Armstrong, et al (1982) are also presented. The results indicate that the frontal speeds decrease with increasing temperature and that the downward frontal speed is consistently larger than the corresponding upward frontal speed.

A model has been developed to characterize the debris bed quench behavior as observed in the experiments. Based upon the above observations it is assumed that the packed bed heat transfer occurred at the quench front during both the downward and upward frontal periods. The rate of heat transfer with liquid supplied from an overlying pool is assumed to be limited by maximum rate at which vapor can be removed from the bed under conditions of countercurrent two-phase vapor-liquid flow in or to the packed bed. A coupled set of equations were developed which include (i) a lumped parameter bed energy equation and (ii) countercurrent flow hydrodynamics equations. Three hydrodynamics models were used to characterize the two phase countercurrent flow processes: (i) the Zuber "CHF" model (Zuber, 1959), (ii) a modified version of the Lipinski debris bed model (Lipinski, 1981) and (iii) a modified version of the Ostenson flooding model (Ostenson, 1981). The set of equations was solved simultaneously for the particle bed heat flux and the downward- and upward-frontal speeds.

The data are compared with model predictions in Figures 4 and 5. Figure 4 indicates that the heat transfer rate is characterized reasonably well by either the CHF model or the TRANSBED (quasi-steady Lipinski) model. The cooling front data shown in Figure 5 agree with the model over the entire range of temperature with the possible exception of the lowest bed temperature.

The results of the program suggest that:

(i) A superheated particle bed quenches in a two-step bi-frontal process. A partial quench front first propagates downward removing a fraction (f_d) of the stored sensible heat of the bed. A second upward-directed quench front starts when the downfront reaches the bed bottom. The upward front removes the balance ($1-f_d$) of the stored energy. Experimental data suggest that f_d = 0.3-0.4.

(ii) The net rate of energy removal from the bed is, within the scatter of the data, independent of initial bed temperature and is identical during both the downward and upward frontal periods.

(iii) The above observations strongly suggest that the phenomenon which limits the net heat removal from a superheated bed is hydrodynamic in nature. This is consistent with the hypothesis that the heat transfer is limited by the hydrodynamics of countercurrent two-phase flow, either just above the bed or within the bed.

Major implications of the results with respect to LWR reactor safety are:

(i) The rate of containment building pressurization resulting from quenching of superheated beds of core debris by overlying pools of liquid would be limited by the hydrodynamics of countercurrent two phase flow to or within the beds. The data and models indicate that this conclusion is independent of initial bed temperature.

(ii) The observed frontal characteristics, however, suggest that the debris ahead of the initial cooling front would remain dry until arrival of the downward front. Attack of the concrete by the hot solid debris must be considered during this time period.

3. HEAT TRANSFER IN CORE-CONCRETE INTERACTIONS

The phenomena of core-concrete interactions impact upon containment integrity of a light water reactor (LWR) following postulated complete meltdown of the core by containment pressurization due to condensable and non-condensable gas generation, possible ignition of combustible gases, and concrete basemat penetration. In order to develop a predictive capability to analyze such complicated interactions, the CORCON code (Muir, 1981) has been developed at Sandia Laboratory under USNRC sponsorship. Modeling of core-concrete interactions involves many poorly understood and complicated heat transfer phenomena for which there exists a sparse data base. In support of the CORCON code, one heat transfer aspect of core-concrete interactions has been investigated which had been found to have significant impact upon the results of generic code calculations, namely the phenomenon of heat transfer between overlying immiscible liquid layers whose interface is agitated by gases liberated from the underlying concrete.

The model used in CORCON to characterize liquid-liquid heat transfer to an interface agitated by transverse gas flow is a correlation developed by Konsetov (1966) to model heat transfer from a horizontal surface with gas injection. Other models which have been applied to liquid-liquid interfacial

heat transfer with bubble agitation are a model by Grief (1965) as well as the surface renewal model of Szekeley (1963). When these models were compared to a limited amount of experimental data taken with an oil-water fluid pair (Werle, 1978), it was found that the models seriously underpredicted both the magnitude and the trend of the heat transfer data, deviating from the data by as much as two orders of magnitude at a superficial gas velocity of only 1 cm/sec. As a result of this poor agreement between the data and the models, a parametric sensitivity analysis was performed to determine the impact of this phenomena upon integrated code calculations of core-concrete interactions.

The effect of interfacial heat transfer was examined parametrically, by increasing the heat transfer coefficient by a factor of 10 and 100, chosen on the basis of comparison of the heat transfer models to the limited experimental data. It was found that the integrated results of the core-concrete interactions were significantly affected by these parametric variations on the interfacial heat transfer coefficient. The Konsetov heat transfer model in CORCON always resulted in an upper bound to the generation rates of combustible, condensable and non-condensable gases from the concrete. However, increasing this magnitude of the coefficient by factors of 10 and 100 reduced these gas generation rates by as much as a factor of from two to five (Greene, 1982).

The reason for this effect on the gas release rates from the concrete is that the downward heat flux into the concrete from the heavy core oxide layer was reduced due to the increased upward heat flux into the overlying lighter metallic layer. This reduced downward heat flux similarly reduced the concrete ablation rate and reduced the rate of dilution of the lower oxide layer by concrete slag. Accompanying the reduced gas generation rates and reduced concrete ablation rate by increasing the interfacial liquid-liquid heat transfer coefficient, it was found that the layer temperatures themselves would decrease significantly faster with the increase in the magnitude of the interfacial liquid-liquid heat transfer coefficient. An example of the reduced gas generation rates and reduced layer temperatures due to enhancing the interfacial heat transfer coefficient is shown in Figure 6a-f. On the basis of these observations, the experimental and analytical program about to be described was performed.

Mercury-Water Bubbling Interfacial Heat Transfer: Non-Entraining

Two sets of bubbling heat transfer data were taken with mercury-water fluid pairs, Series 300 and Series 400 data. The bubble radii were in the range 0.3 to 0.5 cm and the superficial gas velocity was varied over the range from zero to 1.4 cm/sec. These data are presented in Figure 7 along with the Wood's metal-oil data of Werle (1978, 1981). In the limit of zero gas flow rate, these data converged asymptotically to a lower limit calculated by the natural convection model of Haberstroh (1974). As the superficial gas velocity increased, the heat transfer coefficient similarly increased due to the periodic bubble-induced disturbances at the liquid-liquid interface. The vertical temperature distribution demonstrated a sharp gradient in the vicinity of the fluid-fluid interface, suggesting that the interface did maintain its approximate spatial integrity and that mixing and entrainment were absent. These observations were further supported by visual and photographic evidence

of the absence of entrainment of mercury even under intense interfacial disturbance.

The mercury-water heat transfer data were found to be greater in magnitude than the Wood's metal-oil data (Werle, 1978; 1981) by a significant margin. The observed superiority of the water layer to the oil layer in transferring heat is evident from the data in Figure 8 and the ratio is roughly a factor of five increasing to as much as ten. On the basis of the surface renewal formulation shown in Figure 7, this ratio should be approximately four. However, as will become evident in the discussion, there are factors absent from this formulation which, when included, may account for this discrepancy.

The regime of heat transfer between two fluid layers enhanced by interfacial disturbances generated at their interface by rising bubbles with the absence of entrainment is referred to as the surface renewal regime. When the gas flux is initiated, the interfacial heat transfer coefficient is found to increase above the value characteristic of pure steady natural convection. For the mercury-water case, no large scale entrainment of the mercury is observed into the overlying water layer. In this case, the bubble acts only to disrupt the temperature gradients at the interface and transient conduction acts to renew the gradients until the arrival of a subsequent bubble. The mercury-water and Wood's metal-oil data are characterized by the surface renewal model.

The major assumptions of the surface renewal model are that a rising bubble totally destroys the temperature gradients on both sides of the interface only in the area of impact projected by the bubble, no influence is felt outside the bubble area, and surface distrubances do not enhance the transport mechanisms or the interfacial surface area. As is evident from Figure 7, the surface renewal heat transfer model of Szekeley (1963), modified by Blottner (1979),

$$h_{SZE} = 1.69\ k\ (j_g/\kappa r_b)^{1/2} \qquad (1)$$

where k is the thermal conductivity, κ is the thermal diffusivity, and r_b is the bubble radius, represents a lower bound to both the mercury-water data as well as the Wood's metal-oil data. In both cases the deviation between the measured and calculated heat transfer coefficient increases with increasing superficial gas velocity, indicating the effect of the increasing disturbance intensity and interfacial wave propagation on the magnitude of the heat transfer. The fact that the discrepancy is greater for the water-mercury data than for the oil-Wood's metal data may indicate the presence of a Prandtl number effect in addition to the hydrodynamic interfacial stretching mechanism due to surface waves.

Nevertheless, for fluid pairs that do not mix or entrain even under the influence of transverse gas bubbling through their interface, the simple transient conduction surface renewal model is found to predict a lower limit to the magnitude of the interfacial heat transfer coefficient, differing from the measured data by up to a factor of four over the range of conditions cov-

ered by these experiments.

Water-Oil Bubbling Interfacial Heat Transfer: Entraining

In addition to the liquid metal-oil/water interfacial heat transfer experiments which did not exhibit entrainment over the entire range of gas velocity covered, experiments were also performed with zinc sulfate-silicone oil (Series 100) and copper sulfate-silicone oil (Series 200) fluid pairs which demonstrated entrainment and mixing when their interface was agitated by rising bubbles from below. The bubble radii and superficial gas velocity were in the same range as for the liquid metal-oil/water experiments. The data for the Series 100 and 200 oil-water experiments are presented in Figure 8 along with the oil-water data of Werle. These experiments, all experiencing liquid-liquid entrainment effects, are compared to the Wood's metal-oil data previously discussed.

In the limit that the superficial gas velocity asymptotically goes to zero, these data converge to the natural convection limit represented by the Haberstroh model. As the superficial gas velocity was increased, a dramatically different behavior was observed than for the fluid pairs which did not exhibit entrainment. Instead of a gradual increase in magnitude, the heat transfer coefficient is seen to suddenly jump almost a factor of ten at the onset of bubbling and steeply increase until, at a gas velocity of 1 cm/s, it is greater than the silicone oil-Wood's metal data by more than two orders of magnitude. The measured vertical temperature distribution exhibited characteristics of an intermediate mixing zone in which the temperature gradually changed from one layer to the other. This is in contrast to the sharp temperature gradient measured with non-entraining fluids previously. These observations were further supported by visual and photographic evidence of the severe mass entrainment rate even at modest superficial gas velocities below 1 cm/sec.

The significant increase in interfacial heat transfer for the silicone oil-water fluid pair over that measured for the silicone oil-Wood's metal fluid pair (KFK) is attributed directly to the effect of mass entrainment of the hot lower fluid across the interface into the cold upper fluid. This regime of heat transfer is referred to as the entrainment heat transfer regime (Greene, 1982).

As the bubble penetrates the liquid-liquid interface, a finger of the lower heavy fluid is sucked upward into the upper layer in the bubble wake. At some location, this liquid finger is observed to pinch off; the fluid below the point of the break returns downward through the interface, while the fluid above this point continues to entrain upwards in the wake region of the bubble. In the case of large entrained drops, they are also observed to fragment in the vortex region behind the bubble into smaller droplets, greatly increasing the surface area for heat transfer. On the basis of simple analysis of transient convective heat transfer around a sphere, it can be shown that for the conditions of these experiments, the droplets essentially transfer all their excess enthalpy to the upper fluid prior to settling back to the lower fluid layer from whence they came. On the basis of these observations, it is argued that one only need to know the liquid entrainment rate in order to

calculate the entrainment heat transfer rate. In this fashion, the overall heat transfer coefficient can be written as the sum of the interfacial surface renewal contribution and the entrainment contribution as

$$h_{eff} = h_{SZE} + j_2 \rho_2 C_{p2} \qquad (2)$$

where ρ_2 and C_{p2} are the density and specific heat of the entrained phase, respectively, and j_2 is the volumetric entrainment rate of the lower fluid per unit cross sectional area. At present, calculation of the entrainment rate, j_2, is treated parametrically as a function of the gas superficial velocity, $j_2 = C_2 j_g$. In reality it is recognized that C_2 is not a constant but is a function of j_g itself. For this discussion, C_2 is assigned the values 0.3 and 1.0 awaiting further attempts to improve the entrainment rate model which are currently underway in recognition of the obvious nonlinear relationship between j_g and j_2.

The results of the comparison of Equation (2) to the oil-water entrainment data are shown in Figure 8. Note that the choice of C_2 in the range of 0.3 to 1.0 appears to bracket the available data. The development of a more refined entrainment rate model will enable a more mechanistic calculation of entrainment heat transfer rate.

Nevertheless, for fluid pairs that exhibit interfacial mixing and entrainment under the influence of transverse gas bubbling through their interface, a simple entrainment rate heat transfer model is seen to reasonably bracket the available experimental data when appropriate assumptions regarding the mass transfer rate are incorporated. This limitation is expected to be relaxed when a mechanistic entrainment rate model for j_2 is available.

ACKNOWLEDGEMENTS

This work was performed under the auspices of the United States Nuclear Regulatory Commission, Office of Nuclear Regulatory Research, Division of Severe Accident Evaluation.

The authors acknowledge the help of Ms. Linda Hanlon in preparation of this manuscript for publication.

REFERENCES

Armstrong, D. R., D. H. Cho and L. Bova, "Formation of Dry Pockets During Penetration into a Hot Particle Bed," Trans. Am. Nucl. Soc., 41, 418-419 (June 1982).

Blottner, F. G., "Hydrodynamics and Heat Transfer Characteristics of Liquid Pools with Bubble Agitation," SAND 79-1132 (1979).

Greene, G. A. and C. E. Schwarz, "An Approximate Model for Calculating Overall Heat Transfer Between Overlying Immiscible Liquid Layers With Bubble-Induced Liquid Entrainment," Information Exchange Meeting on Post-Accident Debris Cooling, Karlsruhe, Federal Republic of Germany (1982).

Greene, G. A., C. E. Schwarz, J. Klages and J. Klein, "Heat Transfer Between Immiscible Liquids Enhanced by Gas Bubbling," International Meeting on Thermal Reactor Safety, Chicago, Illinois (September 1982).

Grief, R., "Heat Transfer with Gas Injected at the Surface," Int. J. Heat Mass Transfer, 8, pp. 1253-1254 (1965).

Haberstroh, R. D., and R. D. Reinders, "Conducting Sheet Model for Natural Convection Through a Density Stratified Interface," Int. J. Heat Mass Transfer, 17, pp. 307-311 (1974).

Konsetov, V. V., "Heat Transfer During Bubbling of Gas Through Liquid," Int. J. Heat Mass Transfer, 9, pp. 1103-1108 (1966).

Lipinski, R., et al., "Advanced Reactor Safety Research Quarterly Report January-March 1980," Sandia National Laboratories, NUREG/CR-1594, 13, 1, 88 (April 1981).

Meyer, J. F., "Preliminary Assessment of Core Melt Accidents at the Zion and Indian Point Nuclear Power Plants and Strategies for Mitigating Their Effects," Vol. 1, U. S. Nuclear Regulatory Commission Report, NUREG-0850 (November 1981).

Muir, J. F., et al., "CORCON-MOD1: An Improved Model for Molten Core-Concrete Interactions," SAND 80-2415 (1981).

Murfin, W. F., "Report of the Zion/Indian Point Study: Volume 1," Sandia National Laboratory, SAND 80-0617/1 (August 1980).

Ostenson, R. W. and R. J. Lipinski, "A Particle Bed Dryout Model Based on Flooding," Nuc. Sci. & Eng., 79, 110-113 (1981).

Pratt, W. T. and R. A Bari, "Containment Response During Degraded Core Accidents Initiated by Transients and Small Break LOCA in the Zion/Indian Point Reactor Plants," Brookhaven National Laboratory, BNL-NUREG-51415 (July 1981).

Szekeley, J., "Mathematical Model For Heat or Mass Transfer at the Bubble-Stirred Interface of Two Immiscible Liquids," Int. J. Heat Mass Transfer, 6, pp. 417-422 (1963).

Werle, H. "Modellexperimente zum Kernschmelaen," Halbjahresbericht 1978/1, PNS 4332, Kerforschungszentrum Karlsruhe FRG (1978).

Werle, H. "Modellexperimente zum Kernschmelzen-Einfluss eines Gasstroms auf den Warmeubergang Zwischenzwei Flussigkeitsschichten," Halbjahresbericht 1978/2, pp. 4300-79-4300-82, KFK (1978).

Werle, H. "Enhancement of Heat Transfer Between Two Horizontal Liquid Layers by Gas Injection at the Bottom," KFK 3223 (1981).

Wooton, R. O. and H. I. Avci, "MARCH (Meltdown Accident Response Characteristics) Code Description and User's Manual," Battelle Columbus Laboratories, NUREG/CR-1711 (October 1980).

Yang, J. W., "Cooling of Core Debris and the Impact on Containment Pressure," Brookhaven National Laboratory, NUREG/CR-2066 (July 1981).

Zuber, N., "Hydrodynamic Aspects of Boiling," Dissertation, Univ. of California, AECU-4439 (1959).

RECENT PUBLICATIONS AND FORMAL REPORTS

1. Greene, G. A. and C. E. Schwarz, "Interfacial Heat Transfer Between Overlying Liquid Layers with Gas Agitations," Trans. Am. Nucl. Soc., 39, (November 1981).

2. Moszynski, J. R. and T. Ginsberg, "Effect of Dispersed Particulate or Droplet Phase on the Rayleigh-Taylor Instability of a Gas-Liquid Interface," Brookhaven National Laboratory, BNL-NUREG-51533 (March 1982).

3. Ginsberg, T., et al., "Phenomenology of Transient Debris Bed Heat Removal," to be published in proceedings of Information Exchange Meeting on Post-Accident Debris Cooling, Karlsruhe, W. Germany (July 1982).

4. Greene, G. A. and C. E. Schwarz, "An Approximate Model For Calculating Overall Heat Transfer Between Overlying Immiscible Liquid Layers with Bubble-Induced Liquid Entrainment," Information Exchange Meeting on Post Accident Debris Cooling, Karlsruhe, Federal Republic of Germany (July 1982).

5. Ginsberg, T., et al., "Transient Core Debris Heat Removal Experiments and Analysis," Presented at International Meeting on Thermal Nuclear Reactor Safety, Chicago, Illinois (August 1982).

6. Greene, G. A., "Experimental and Analaytical Study of Natural Convection Heat Transfer of Internally Heated Liquids," Ph.D. Thesis, BNL-NUREG 51585, NUREG/CR 2939 (August 1982).

7. Greene, G. A., C. E. Schwarz, J. Klages and J. Klein, "Heat Transfer Between Immiscible Liquids Enhanced by Gas Bubbling," International Meeting on Thermal Nuclear Reactor Safety, Chicago, Illinois (August 1982).

8. Greene, G. A., T. F. Irvine, Jr. and O. C. Jones, Jr., "Experimental and Analytical Study of Natural Convection Heat Transfer of Internally Heated Fluids," Seventh International Heat Transfer Conference, Munich, Federal Republic of Germany (September 1982).

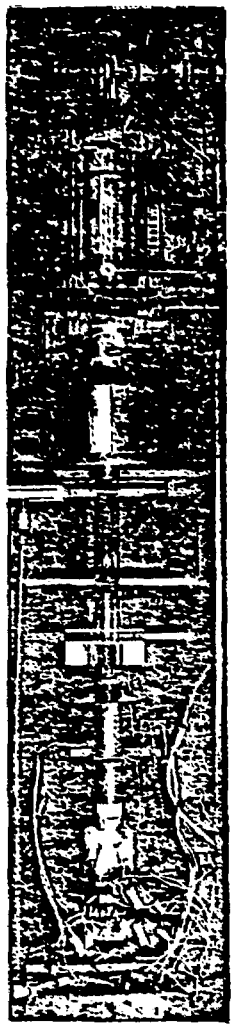

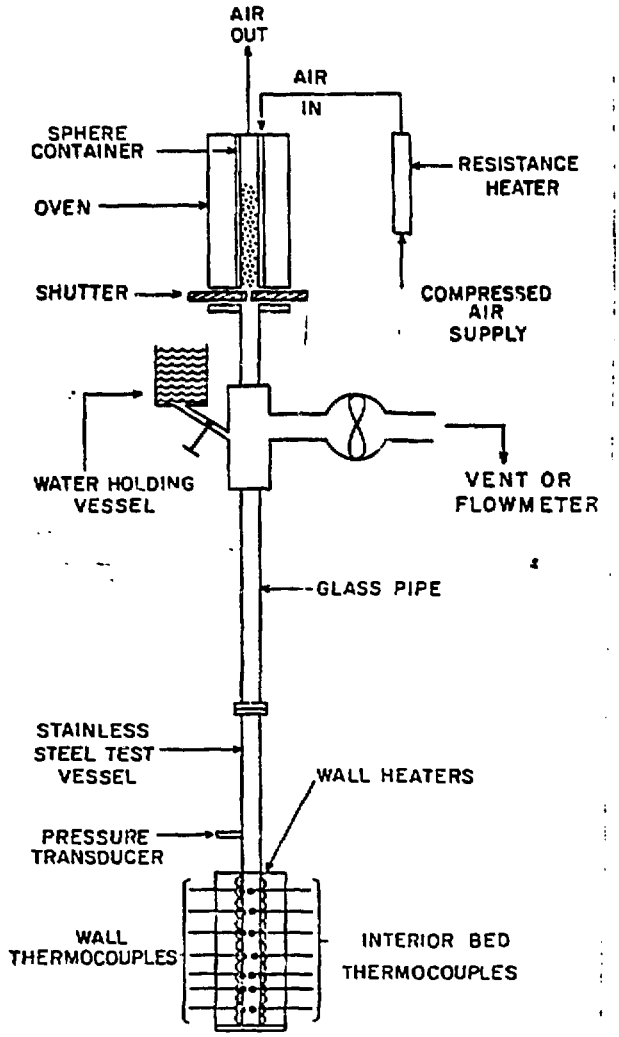

(a) (b)

FIGURE 1-(a) Photograph and (b) Schematic Diagram of Test Apparatus

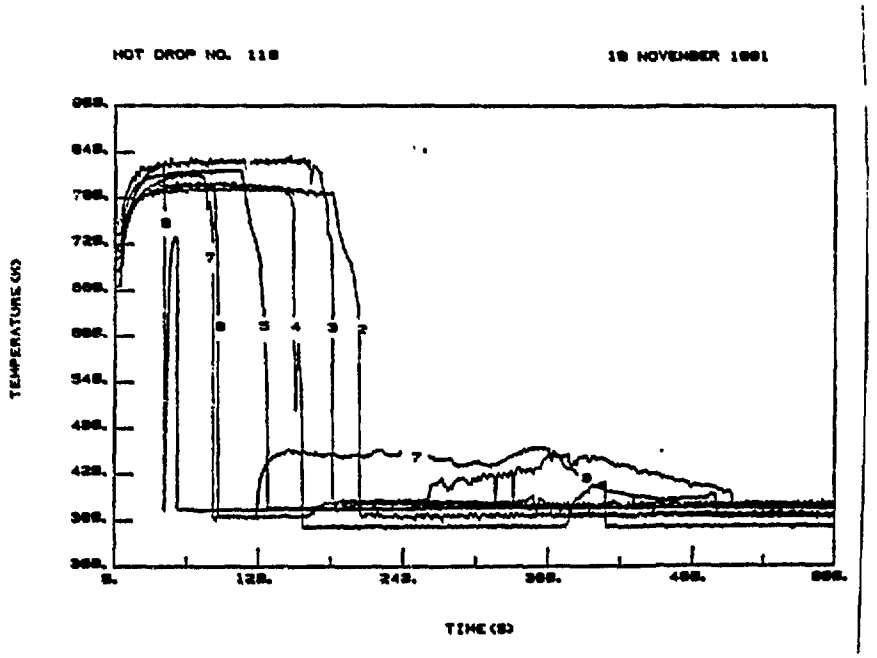

FIGURE 2 - Bed Temperature Traces: T_0=800K; Bed Height-327 mm

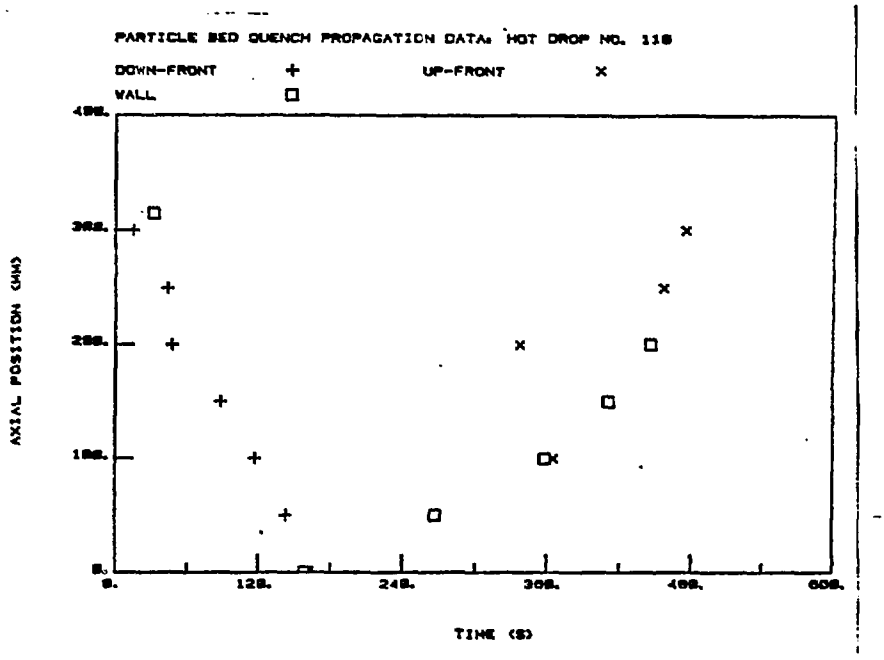

FIGURE 3 - Frontal Propagation Results: T_0=800K; Bed Height=327 mm

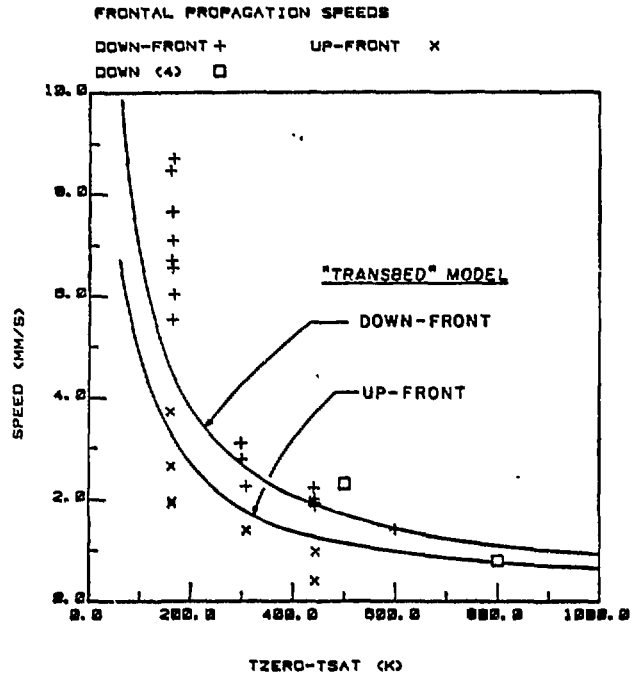

FIGURE 4 - Frontal Progression Speeds

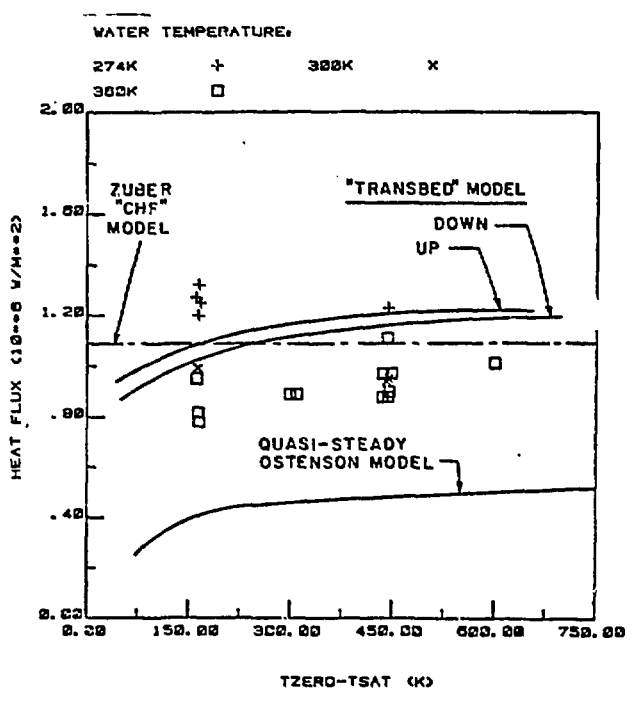

FIGURE 5 - Particle Bed Heat Transfer Rate: Measured and Calculated

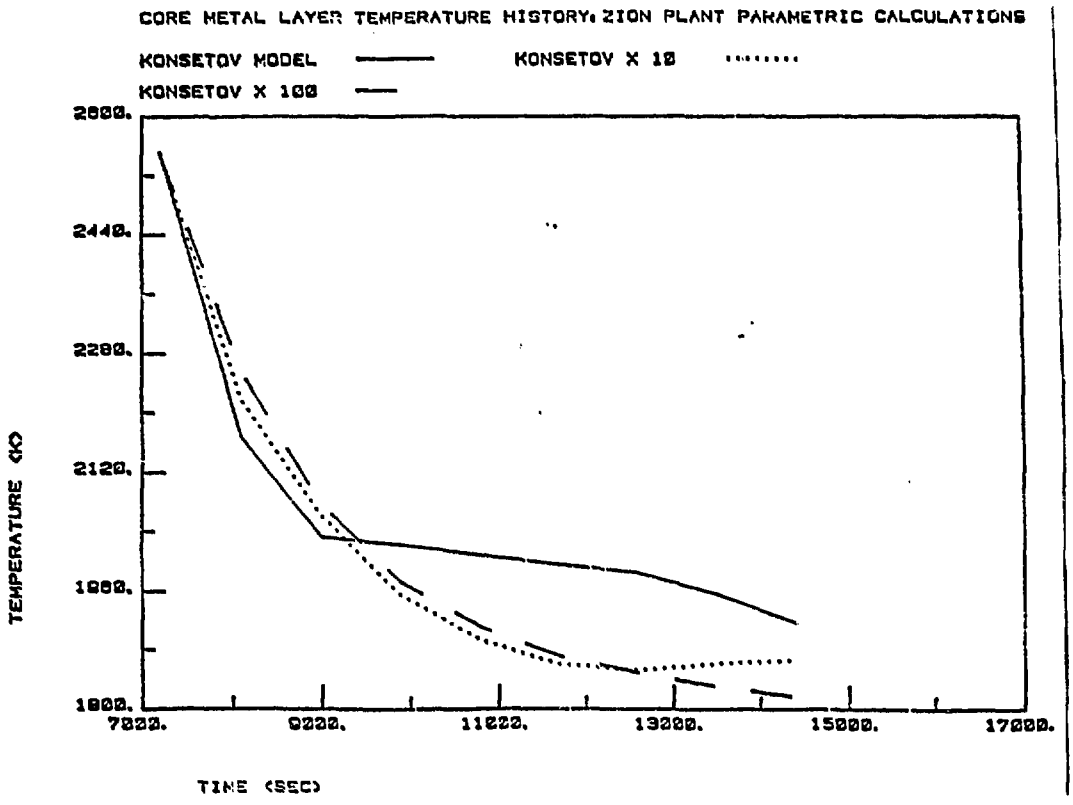

FIGURE 6a

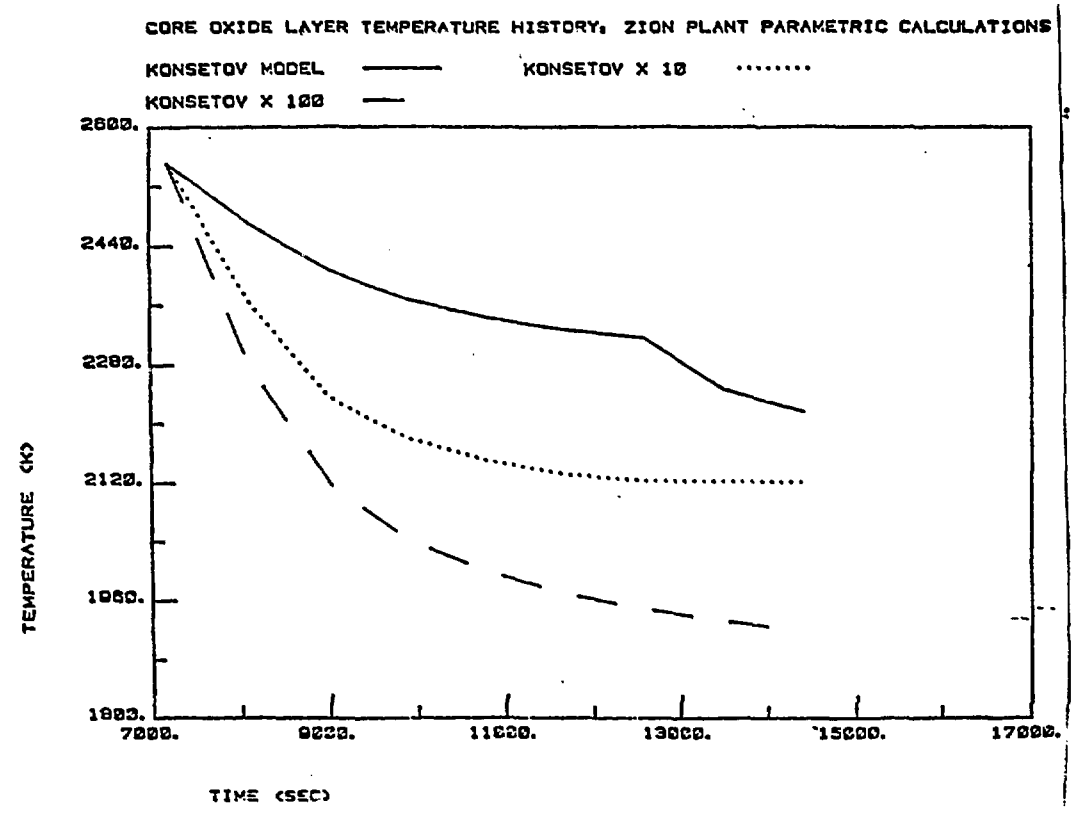

FIGURE 6b

FIGURES 6a-f - Sensitivity of CORCON Calculations to Interfacial Liquid-Liquid Heat Transfer

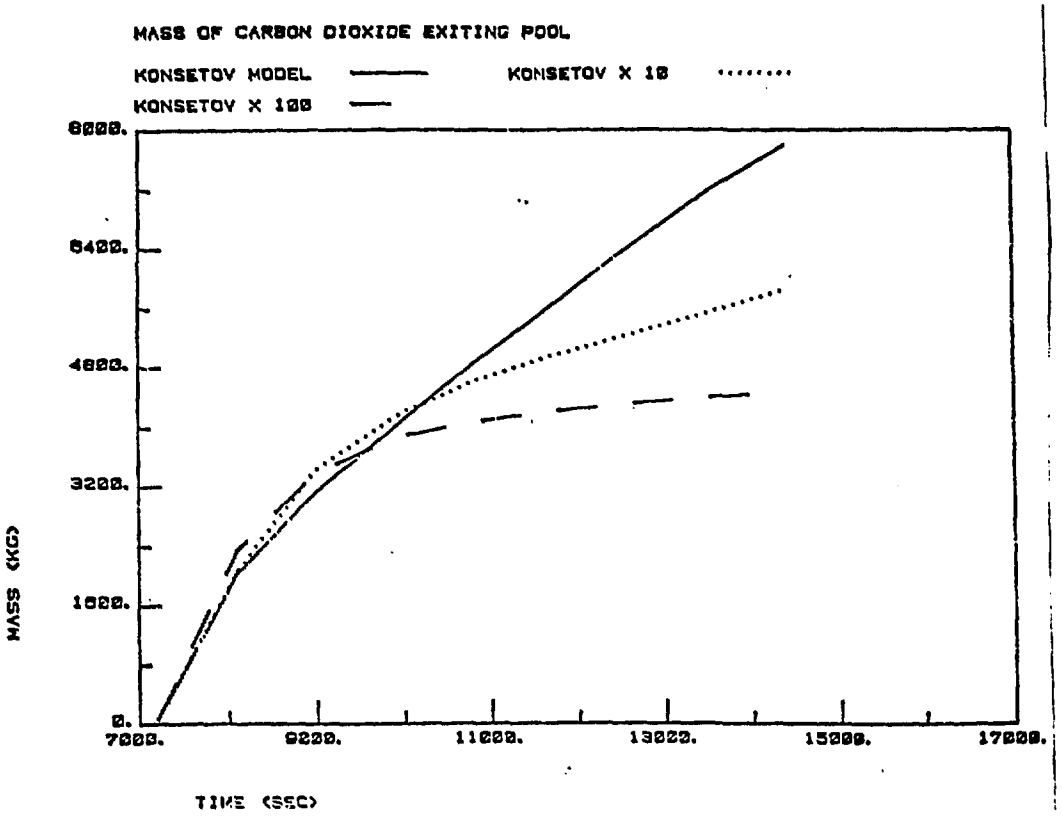

FIGURE 6c

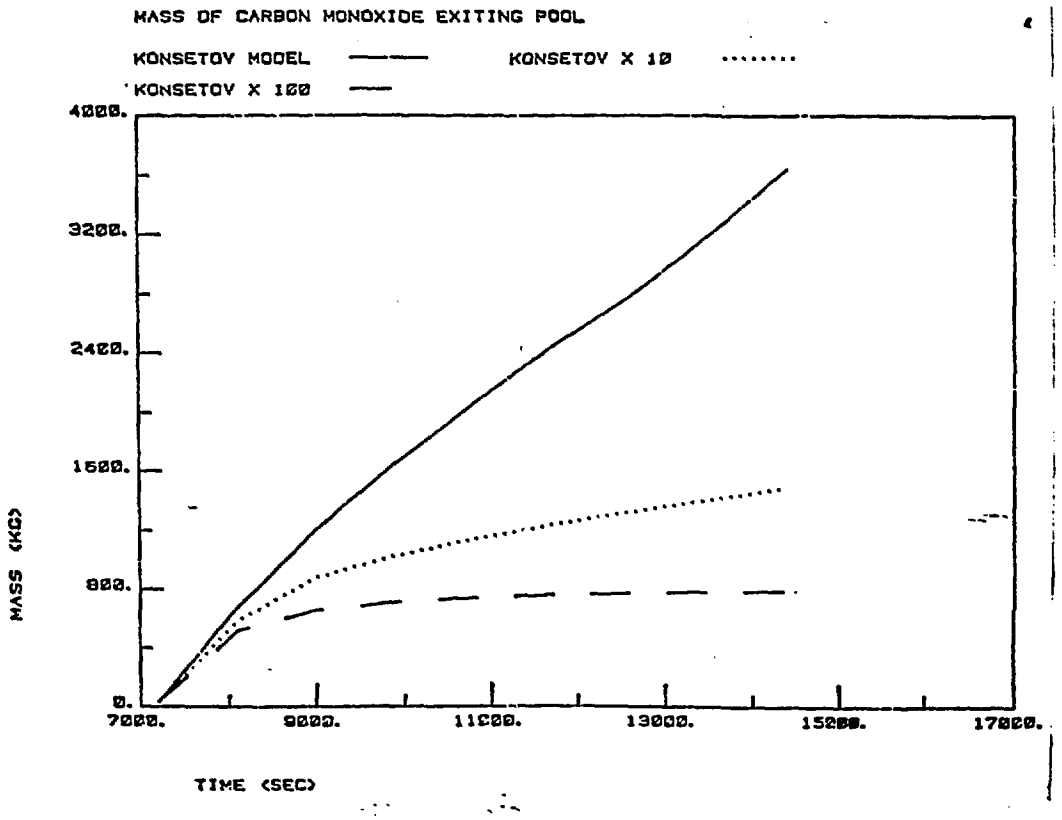

FIGURE 6d

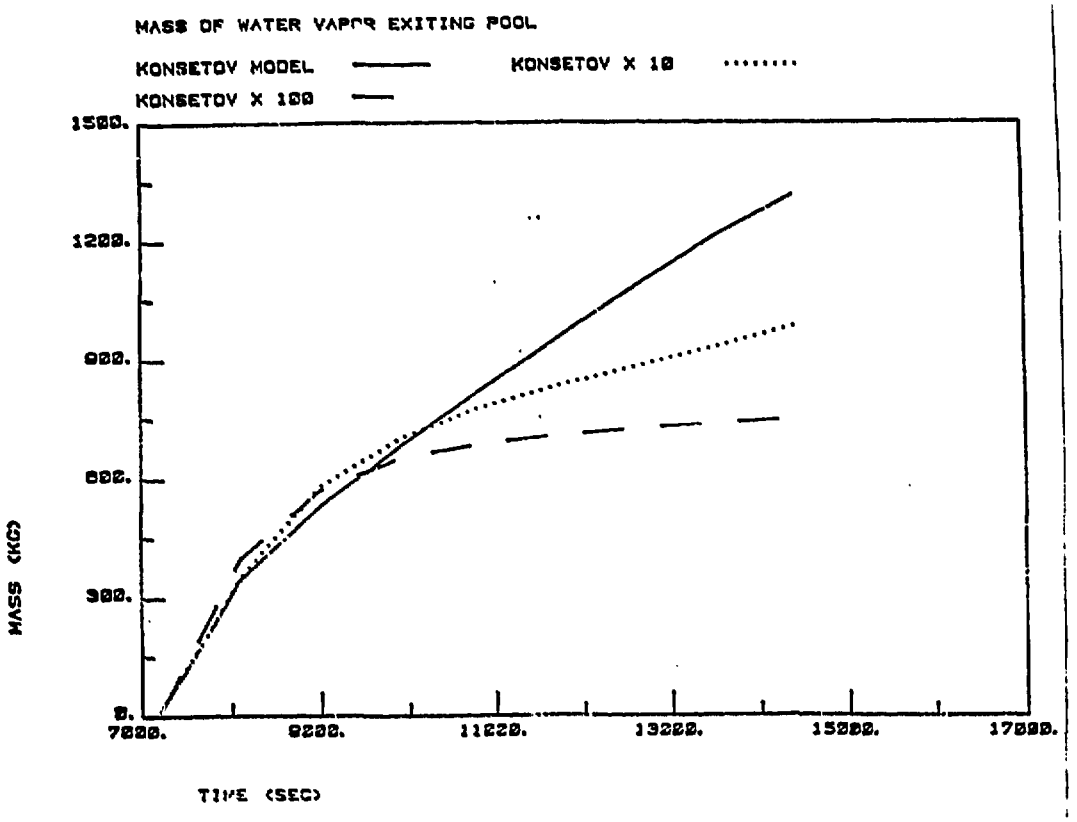

FIGURE 6e

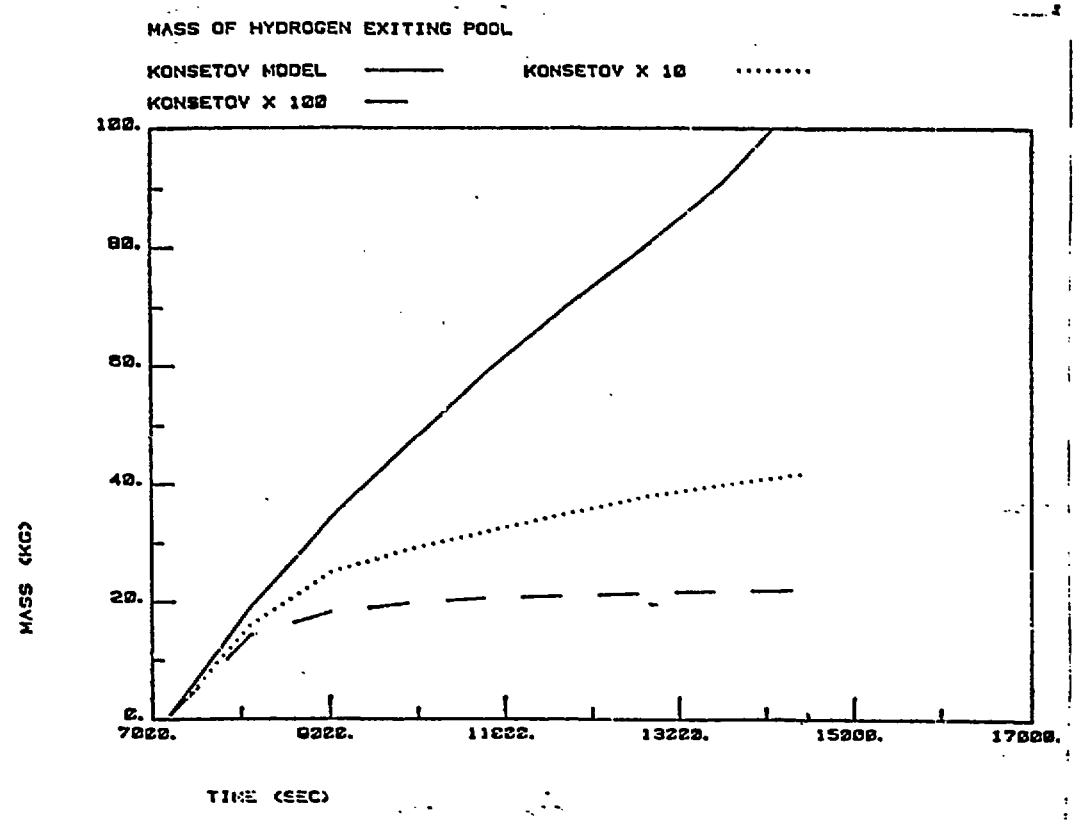

FIGURE 6f

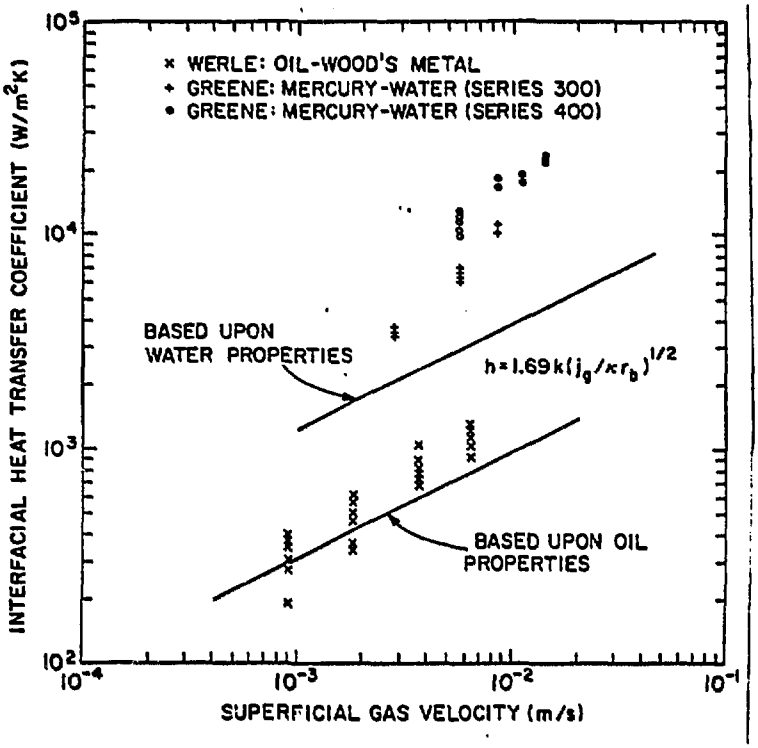

FIGURE 7 - Interfacial Heat Transfer Coefficient vs. Superficial Gas Velocity: Non-Entrainment Regime

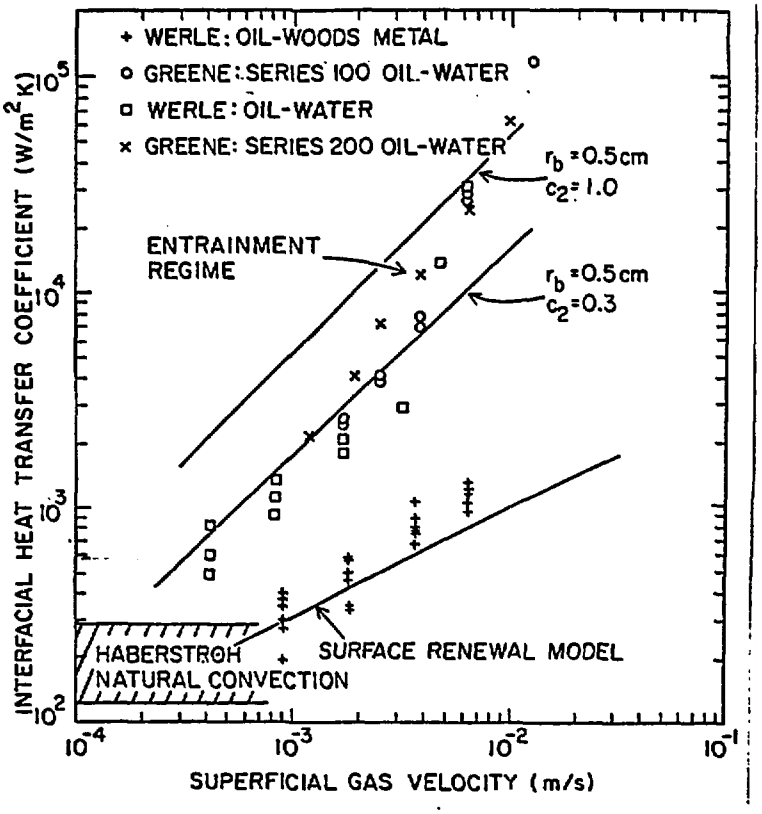

FIGURE 8 - Interfacial Heat Transfer Coefficient vs. Superficial Gas Velocity: Entrainment Regime